Stochastic Frequency-Security Constrained Scheduling of a Microgrid Considering Price-driven Demand Response

Vahedipour-Dahraie, Mostafa; Rashidizadeh-Kermani, Homa ; Anvari-Moghaddam, Amjad; Guerrero, Josep M.

Published in:
Proceedings of the 2018 International Symposium on Power Electronics, Electrical Drives, Automation and Motion (SPEEDAM)

DOI (link to publication from Publisher):
10.1109/SPEEDAM.2018.8445233

Publication date:
2018

Stochastic Frequency-Security Constrained Scheduling of a Microgrid Considering Price-Driven Demand Response

Mostafa Vahedipour-Dahraie and Homa Rashidizadeh-Kermani
Department of Electrical & Computer Engineering
University of Birjand
Birjand, South Khorasan, Iran
{vahedipour_m, rashidi_homa}@birjand.ac.ir

Amjad Anvari-Moghaddam and Josep M. Guerrero
Department of Energy Technology
Aalborg University
9220 Aalborg East, Denmark
{aam,joz}@et.aau.dk

***Abstract*—This paper proposes a two-stage stochastic model for optimal frequency-security constrained energy and reserve scheduling in an islanded residential microgrid (MG) with price-responsive loads. Based on this model, scheduling of the controllable units in both supply and demand sides is done in a way not only to maximize the expected profit of MG operator (MGO), but also to minimize the energy payments of customers. To study the effect of uncertain parameters and demand-side participation on system operating conditions, an AC-optimal power flow (AC-OPF) approach is also applied. The proposed stochastic optimization model is then applied to a typical islanded MG and its effectiveness is demonstrated through different scenarios. Simulation results show that participation of customers in price-driven demand response (DR) programs can reduce energy consumption cost of customers while improving the MG frequency response in steady state.**

Keywords— Demand response (DR), Frequency-Security, Reserve scheduling, Renewable energy resources (RESs)

I. INTRODUCTION

In recent years, demand-side management (DSM) has been contemplated as a crucial option in most energy policy decisions. In restructured power systems, the scope of DSM has also been considerably expanded to include demand response (DR) programs [1], to provide many potential benefits such as reduction of operation cost and emission [2], improvement of system reliability [3]-[4], shaping of daily load profile [5] as well as providing financial incentives to customers to benefit from lower hourly demands [6].

The advent of microgrids (MGs) in modern power systems has provided a high potential to facilitate the active participation of end-use consumers in DR programs [7]. However, due to the increasing penetration level of renewable resources such as wind and solar, it is necessary to efficiently manage operation of such systems in presence of uncertainties [8]. This is even more important in islanded MGs where there is lower inertia (compared to conventional power systems with high inertia provided by synchronous machines) and higher risk of stability issues [9]-[10]. Thus, the operational security of MG is a great challenge (especially in the presence of uncertainties) that should be investigated accurately. Frequency as a key control variable represents the MG security, properly. The relation between frequency and energy and reserve scheduling enables the MG central controller (MGCC) to apply proper energy management mechanisms to keep the MG security in a cost-effective manner. With the application of DR programs, MGCC can manage the responsive loads not only to reduce energy costs, but also to provide the MG frequency security in a more reliable and economical manner [11]. The effects of DR programs on day-ahead energy and reserve scheduling in islanded MGs considering both security and economic goals are studied in a few works [12]-[15]. For example, a stochastic multi-objective framework is proposed in [12] for joint energy and reserve scheduling in day-ahead, but it does not consider AC network, voltage security, load and wind power uncertainties. In [13], authors addressed the problem of the probabilistic steady-state analysis of an electrical distribution system that includes wind and photovoltaic power plants. A new method is presented that takes into account the uncertainties due to the time variations of power load demands and the random nature of solar and wind energy. Also, in [14] a stochastic scheduling of microgrids is proposed that energy exchange with the macrogrid is coordinated ahead of time. A scheduling problem is formulated for a microgrid system and chance-constrained optimization is used to minimize operational cost and ensure the energy exchange commitments are met. Also, an energy management strategy is proposed in [15] to coordinately manage the DR resources and generation units in a way to meet the frequency security requirements. However, in none of the reviewed literatures, the effect of real time pricing (RTP)-based DR programs on frequency security is reported. Also, an economic-based DR model based on consumers' preferences is not investigated.

In this paper, a scenario-based two-stage stochastic programming is developed to model the effects of MG uncertainties on energy and reserve management. Different DR actions enabled under RTP scheme are also investigated and their effects on the frequency deviations in a residential islanded MG are studied. Furthermore, an AC-optimal power flow (AC-OPF) approach is applied to model the actual operating conditions and to assess the influence of DR resources on frequency security.

II. Model Description

In this work, MGCC is responsible for energy and reserve scheduling of the residential MG in islanded mode. The MG operator (MGO) monitors the optimization process and has a supervisory control on decisions. It is also assumed that the customers are equipped with in-home energy management controllers and several smart household appliances. Due to different location of customers in the network, N_J groups of loads are also considered for evaluating the influence of participation in DR programs. The participation level (percentage) of each group of customers in DR program is represented with coefficient η. Customers participate in DR programs using two general categories of devices including shiftable and sheddable loads [16]. In load shedding scheme, customers would apply energy efficiency as an alternative to reduce their hourly electricity usage without shifting it to other hours. Shiftable loads are also related to such consumption units that must be run in the course of a day however there is no specific run time for them. In the examined environment, the hourly meteorological information (e.g., wind speed, and solar irradiation) and load level required for scheduling purposes are estimated based on the methods presented in [17]. The energy and reserve scheduling is also done by the MGCC in a way to maximize the MGO expected profit and to minimize consumers' bills while fulfilling the MG securities and technical constraints.

A. Scenario Generation and Reduction

The uncertainty of renewable generation, load and demand elasticity are considered as stochastic variables in this study and their forecasting errors are modeled as a continuous probability density function (PDF). It is assumed that each of the stochastic variables is a zero-mean normal distribution with different standard deviation error and various probabilities dedicated to each interval. Roulette wheel mechanism (RWM) is also used to generate stochastic renewable generation and load reduction scenarios over the examined period [18]. In the next step, K-means algorithm [19] is applied to reduce the computational burden of the stochastic procedure by eliminating the scenarios with very low probabilities and those that are very similar.

B. Economic Model of DR

Each group of consumers that participate in DR programs can modify the consumption pattern based on load shifting/shedding mechanisms. Adding the non-sheddable loads to the consumption mix, the total demand can be calculated as:

$$D_t = \sum_{j=1}^{N_J} \left[D_{j,t}^{NDR} + D_{j,t}^{CDR} + D_{j,t}^{SDR} \right] \tag{1}$$

where, $D_{j,t}^{NDR}$, $D_{j,t}^{CDR}$ and $D_{j,t}^{SDR}$ represent the non-sheddable, sheddable and shiftable loads of group j, at hours t, respectively. The benefit of group j, for single period elastic loads (i.e., sheddable loads) can be calculated as:

$$S(D_{j,t}^{CDR}) = B(D_{j,t}^{CDR}) - D_{j,t}^{CDR}.\rho_{j,t} \tag{2}$$

where, $\rho_{j,t}$ is the electricity price offered to customers j, $S(D_{j,t}^{CDR})$ and $B(D_{j,t}^{CDR})$ are benefit and income of group j at period t after implementing DR only with sheddable loads, respectively. To maximize the benefit of group j, the following criteria must be met.

$$\frac{\partial S(D_{j,t}^{CDR})}{\partial D_{j,t}^{CDR}} = \frac{\partial B(D_{j,t}^{CDR})}{\partial D_{j,t}^{CDR}} - \rho_{j,t} = 0 \tag{3}$$

Based on a quadratic model of DR, the utility of group j of customers is obtained as:

$$B(D_{j,t}^{CDR}) = B_{j,t}^{0} + \frac{\rho_{j,t}^{0}\, D_{j,t}^{CDR}}{1+E_{j,t,t}^{-1}} \times \left[\left(\frac{D_{j,t}^{CDR}}{D_{j,t}} \right)^{E_{j,t,t}^{-1}} - 1 \right] \tag{4}$$

where, $E_{j,t,t}$ is the self-elasticity of load j, $B_{j,t}^{0}$ and $\rho_{j,t}^{0}$ are the initial value of income and electricity price associated with customers of group j, respectively. Differentiating (4) with respect to $D_{j,t}^{CDR}$ and substituting it into (3) gives:

$$\left(1+E_{j,t,t}^{-1}\right) \times \frac{\rho_{j,t}^{0}}{\rho_{j,t}} = \left(\frac{D_{j,t}^{CDR}}{D_{j,t}} \right)^{E_{j,t,t}^{-1}} - 1 + E_{j,t,t}^{-1} \cdot \left(\frac{D_{j,t}^{CDR}}{D_{j,t}} \right)^{E_{j,t,t}^{-1}} \tag{5}$$

Therefore, the consumption of group j at time t is obtained as follows:

$$D_{j,t}^{CDR} = D_{j,t} \cdot \left(\frac{\rho_{j,t}}{\rho_{j,t}^{0}} + \frac{1}{1+E_{j,t,t}^{-1}} \right)^{E_{j,t,t}} \tag{6}$$

Furthermore, shiftable loads are modeled based on cross-elasticity which are defined as demand sensitivity of the t-th period with respect to the price elasticity at h-th period and can be written as [20]:

$$E_{j,t,h} = \frac{\rho_{j,h}^{0}}{D_{j,t}^{0}} \cdot \frac{\partial D_{j,t}}{\partial \rho_{j,h}} \tag{7}$$

where, $E_{j,t,h}$ is the cross-elasticity and $D_{j,t}^{0}$ is the initial value of demand of group j. The amount of shiftable loads after DR using cross-elasticity and applying quadratic function can be obtained as:

$$D_{j,t}^{SDR} = D_{j,t} \cdot \prod_{\substack{t=1 \\ t\neq h}}^{N_T} \left(\frac{\rho_{j,h}}{\rho_{j,h}^{0}} + \frac{1}{1+E_{j,t,h}^{-1}} \right)^{E_{j,t,h}} \tag{8}$$

When the customers participate in DR with both options (i.e., sheddable and shiftable loads), their responsive load is obtained with the summation of (6) and (8) as follows:

$$D_{j,t}^{DR} = D_{j,t} . \exp \sum_{h=1}^{N_T} E_{j,t,h} . \ln \left(\frac{\rho_{j,h}}{\rho_{j,h}^{0}} + \frac{1}{1+E_{j,t,h}^{-1}} \right) \tag{9}$$

III. Problem Formulation

In the proposed optimization framework, the aim is to optimally manage the system supply and demand sides in such a way to maximize the expected profit of the MGO and to minimize the customers' payments considering different constraints. In this regards, a network-constrained day-ahead market clearing model including a two-stage stochastic programming is developed. In the first stage, the energy and reserve resources are scheduled jointly and in the second stage, the MG operational aspects are formulated using scenario-dependent variables.

A. Objective function

As described earlier, the objective function can be presented as:

$$
Max\left[\begin{array}{l}
\sum_{t=1}^{N_T}\{\sum_{j=1}^{N_J}\rho_{j,t}.D_{j,t} \\
-\sum_{i=1}^{N_G}\left[C(P_{i,t})+(C_{i,t}^{R^U}.R_{i,t}^{U}+C_{i,t}^{R^D}.R_{i,t}^{D}+C_{i,t}^{R^{NS}}.R_{i,t}^{NS})\right] \\
-\sum_{j=1}^{N_J}(C_{j,t}^{R^U}.R_{j,t}^{U}+C_{j,t}^{R^D}.R_{j,t}^{D})-\sum_{w=1}^{N_W}\rho_{w,t}.P_{w,t}-\sum_{v=1}^{N_V}\rho_{v,t}.P_{v,t}\} \\
-\sum_{s=1}^{N_S}\pi_s.\sum_{t=1}^{N_T}\{\sum_{i=1}^{N_G}\left[SUC_i.y_{i,t,s}+SDC_i.z_{i,t,s}\right. \\
\left.+\rho_{i,t}^{Dep}.(r_{i,t,s}^{U}+r_{i,t,s}^{NS}-r_{i,t,s}^{D})\right] \\
-\sum_{j=1}^{N_J}[\rho_{j,t}^{Dep}.(r_{j,t,s}^{U}-r_{j,t,s}^{D})+VOLLEENS_j]\}
\end{array}\right] \tag{10}
$$

where, $(.)_{.,t,s}$ denotes at time t in scenario s. i, w, v and j are indices of DGs, wind turbine, PV unit and load, respectively. $C(P_{i,t})$ is cost of power production of DG i, R represents allocated reserve, $C_{i,t}^{R^U}$, $C_{i,t}^{R^D}$ and $C_{i,t}^{R^{NS}}$ represent bid of up, down and non-spinning reserves submitted by DG i, respectively. $C_{j,t}^{R^U}$ and $C_{j,t}^{R^D}$ represent bid of up and down-spinning reserves submitted by customers j, $\rho_{w,t}$ and $\rho_{v,t}$ represent cost of wind and PV energy, $r_{i,t,s}^{U}$ ($r_{j,t,s}^{U}$) is the up-spinning reserves and $r_{i,t,s}^{D}$ ($r_{j,t,s}^{D}$) is the down-spinning reserve deployed by DG i (load j), $SDC_{i,t}$ ($SUC_{i,t}$) is shut-down (start-up) cost of unit i, $\rho_{i,t}^{Dep}$ ($\rho_{j,t}^{Dep}$) is buying (selling) real-time price offered to unit i (load j). Moreover, in the above equation, the first line represents the revenue of selling energy to customers. The second line is the cost of DG units and their scheduled reserve costs. The third line represents costs of scheduled reserve loads and costs associated with energy provided by wind and PV units. The fourth line represents the costs associated with energy provided by wind and PV units. Moreover, the fifth line denotes the start-up/shut-down costs of DG units at scenarios. The sixth line is the cost of deploying reserves from DG units. Finally, the last line represents the cost of deploying reserves from loads in real-time and the cost of expected energy not served (EENS) for the inelastic loads. VOLL in this line represents the value of lost load.

B. Constraints of the Problem

The constraints of the problem consist of first-stage and second-stage constraints. The first-stage constraints are associated with the capacity cost and do not depend on any specific scenario, while, the second-stage constraints are scenario-dependent and account for stochastic operating conditions. The first-stage constraints expressing as follows:

$$\sum_{i:(i,n)\in M_I(t)}P_{i,t}+\sum_{w:(w,n)\in M_W(t)}P_{w,t}+\sum_{v:(v,n)\in M_V(t)}P_{v,t}-\sum_{j:(j,n)\in M_L(t)}D_{j,t,s}=\sum_{r:(n,r)\in\Lambda(t)}f_{n,r,t}^{P} \tag{11}$$

$$\sum_{i:(i,n)\in M_I(t)}Q_{i,t}+\sum_{w:(w,n)\in M_W(t)}Q_{w,t}+\sum_{v:(v,n)\in M_V(t)}Q_{v,t}-\sum_{j:(j,n)\in M_L(t)}Q_{j,t}=\sum_{r:(n,r)\in\Lambda(t)}f_{n,r,t}^{Q} \tag{12}$$

Equation (11)-(12) represent the active and reactive power (Q) balance in MG in steady state, in which $f_{n,r,t}^{P}$ and $f_{n,r,t}^{Q}$ are active and reactive power flows from bus n to bus r at time t, respectively. The real power generation and the reserve provided by DG units are constrained by (13)-(15).

$$P_{i,t}\le P_i^{\max}u_{i,t}-R_{i,t}^{U}\ ;\ P_{i,t}\ge P_i^{\min}u_{i,t}+R_{i,t}^{D} \tag{13}$$

$$0\le R_{i,t}^{U}\le R_{i,t}^{U,\max}u_{i,t}\ ;\ 0\le R_{i,t}^{D}\le R_{i,t}^{D,\max}u_{i,t} \tag{14}$$

$$0\le R_{i,t}^{NS}\le R_{i,t}^{NS,\max}(1-u_{i,t}) \tag{15}$$

The demand-side constraints determine the degree of participation of each group of customers in energy and reserve scheduling. Here, the residential loads are categorized in different groups based on their location and response type in different buses. For each group, the following criteria must be met:

$$D_{j,t}^{\min}\le D_{j,t}\le D_{j,t}^{\max} \tag{16}$$

$$0\le R_{j,t}^{U}\le D_{j,t}-D_{j,t}^{\min}\ ;\ 0\le R_{j,t}^{D}\le D_{j,t}^{\max}-D_{j,t} \tag{17}$$

By providing up- and down- reserve, the customers are committed to decrease and increase their consumption, respectively. The logic constraints of unit commitment are represented as follow:

$$y_{i,t}-z_{i,t}=u_{i,t}-u_{i,t-1} \tag{18}$$

$$y_{i,t}+z_{i,t}-1\le 0 \tag{19}$$

where, $u_{i,t}$ represents commitment status of DG i {0, 1} and $y_{i,t}$ and $z_{i,t}$ are startup and shutdown indicators of DG i, respectively. The constraint (18) determines the start-up/shut-down status of units, while (19) states that a unit cannot start-up and shut-down during the same period.

The second-stage constraints are similar to the first-stage constraints.

IV. Simulation and Numerical Results

The simulations are performed in a typical low-voltage MG which is depicted in Fig. 1. The MG is operated in the islanded mode and contains five droop-controlled DG units, namely, two micro-turbines (MT1 & MT2), two fuel cells (FC1 & FC2), and one gas engine (GE). The data associated with the installed generation units is extracted from [15]. Additionally, three similar WTs, each with a capacity of 80 kW are installed at buses 6, 9, and 16 and two similar PV plants, each with a capacity of 70 kW. Besides, the MG feeds eight three-phase balanced aggregated loads (Loads 1-8 in Fig. 1) that are equipped with proper controllers to participate in DR programs. All loads are also assumed to be operated at lagging power factor of 0.95. The forecast power of WT and

PV units and also, the total demand load of MG are shown in Fig. 2, [20].

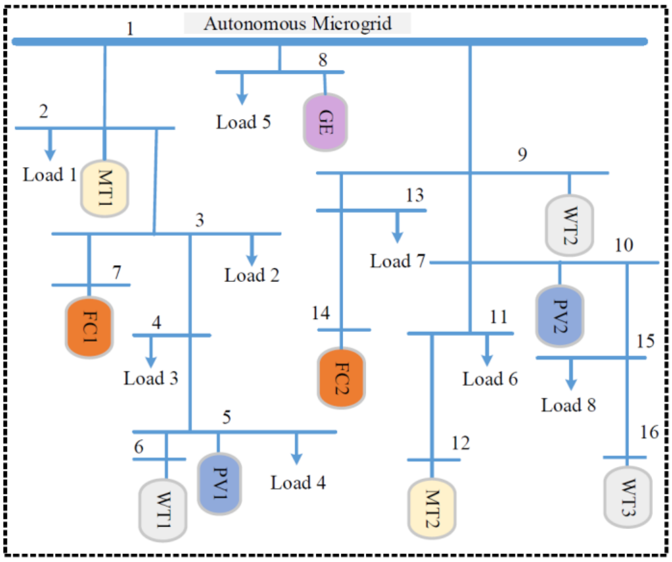

Fig. 1. Single line diagram of the simulated autonomous microgrid.

The load profile has been created by aggregating the electricity demands of 200 residential homes. The price elasticity of total demand is obtained from [20]. Moreover, the hourly time-varying energy price for the study period is also shown in Fig. 3. Also, the value of lost load (VOLL) is assumed to be 1 \$/kWh. To simulate the environmental/behavioral uncertainties within the system, 2000 initial scenarios are generated based on PDFs to represent forecast errors of wind speed, solar irradiation and demand-side contribution. Also, standard deviation of forecast errors of the wind speed, solar irradiation and load demand are considered ±10%, ±10%, and ±20%, respectively [20]. Here, the PDFs are divided into seven discrete intervals with different probability levels. In the next step, by implementing an efficient scenario reduction algorithm, 25 scenarios are selected that represents well enough the uncertainties. Then, the reduced scenarios are applied to the proposed MIP-based optimization model to maximize the expected profit of islanded MGO while considering system voltage and frequency security constraints. The optimization is carried out by CPLEX solver using GAMS software on a PC with 4 GB of RAM and Intel Core i7 @ 2.60 GHz processor. In order to analyze the effect of RTP program on frequency response of MG in steady-state and in different consumers' consumption patterns, the residential devices are divided in three categories and studied in four case-studies.

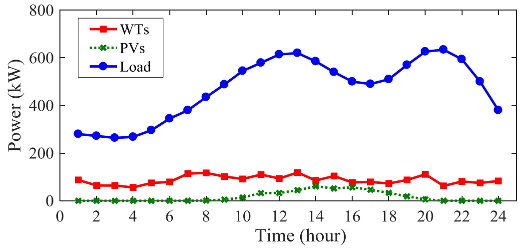

Fig. 2. The output power of WTs, PVs and total demand load of MG.

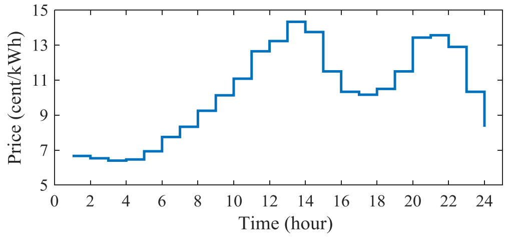

Fig. 3. Hourly energy price (RTP).

In case 1 which is considered as the base case scenario, it is assumed that the loads are not responsive, so there is no contribution from the demand side. In case 2, only DR actions based on sheddable loads are considered while in case 3, DR programs based on load shifting capabilities are studied. Finally, case 4, describes the situation in which the customers participate in RTP-based DR programs using both load shedding and shifting mechanisms.

The optimal values of the expected profit of MGO, customers' payments and cost of DG units have been listed in Table I for the examined scenarios. These values have been obtained for a 24-hour scheduling horizon with regard to the system's economic objectives and constraints as mentioned earlier. As can be observed from Table 1, with increasing customers' participation in DR programs in different working conditions, the expected profit is increased. The reason is that the expensive units are not dispatched to meet the demand of peak periods as the peak loads are decreased by shifting/shedding activities. Moreover, higher contributions in DR activities result in lower customers' bills in all cases. As an example, with 40% DR contribution, the reductions of consumers' bills in cases 2, 3 and 4 are 2.8%, 2.9% and 5.7%, respectively. Moreover, as can be seen in Table I, the operational costs of DGs are reduced significantly with DR actions. For example, by enabling 40% of DR activities, the

TABLE I. THE OPTIMAL VALUES OF THE OBJECTIVE FUNCTION IN DIFFERENT CASES

η (%)	**Expected profit (\$)**				**Customers' payments as bills (\$)**				**Cost of DG units (\$)**			
	Case 1	*Case 2*	*Case 3*	*Case 4*	*Case 1*	*Case 2*	*Case 3*	*Case 4*	*Case 1*	*Case 2*	*Case 3*	*Case 4*
0	229.09	-	-	-	1236.23	-	-	-	835.52	-	-	-
10	-	292.27	296.42	307.96	-	1227.63	1227.20	1218.60	-	819.70	820.69	813.36
20	-	303.21	304.40	320.21	-	1219.03	1218.17	1200.96	-	808.74	813.17	798.13
30	-	310.27	313.07	333.75	-	1210.42	1209.14	1183.33	-	801.76	807.79	786.04
40	-	324.27	319.57	347.62	-	1201.82	1200.11	1165.69	-	795.17	800.57	773.75
50	-	331.66	324.59	363.71	-	1193.22	1191.00	1148.06	-	787.43	795.49	756.75
60	-	340.46	325.27	379.68	-	1184.61	1182.05	1130.43	-	780.16	799.24	746.29
70	-	347.65	323.87	382.56	-	1176.01	1173.01	1112.80	-	772.37	799.47	744.92

TABLE II. COST OF SCHEDULED AND DEPLOYED RESERVES OF MG IN DIFFERENT CASES

η (%)	Case 2				Case 3				Case 4			
	Scheduled reserve cost ($)		Deployed reserve cost ($)		Scheduled reserve cost ($)		Deployed reserve cost ($)		Scheduled reserve cost ($)		Deployed reserve cost ($)	
	DGs	*DR*	*DGs*	*DR*	*DGs*	*DR*	*DGs*	*DR*	*DGs*	*DR*	*DGs*	*DR*
10	115.05	44.92	-98.71	0.30	118.35	42.39	-99.42	-4.01	121.84	39.23	-103.44	-5.44
20	114.17	44.98	-94.43	-4.46	116.95	44.10	-95.03	-9.80	117.42	43.05	-90.26	-17.26
30	113.61	44.74	-90.76	-8.73	119.87	42.46	-93.91	-15.72	117.17	43.41	-78.86	-31.99
40	120.01	38.87	-97.32	-10.79	117.97	44.93	-84.56	-25.44	116.99	44.68	-64.75	-50.60
50	118.85	39.29	-92.71	-15.63	117.10	45.88	-77.35	-33.65	117.44	44.51	-64.68	-51.70
60	120.47	37.76	-92.97	-18.15	114.45	48.96	-77.56	-39.09	117.94	44.79	-68.64	-55.92
70	119.11	38.38	-87.36	-23.78	112.96	51.78	-76.84	-41.04	119.28	46.11	-67.41	-62.87

daily cost of DGs is decreased from 835.52 $ in case 1 (no DR) to $795.17 $, 808.57 $ and 773.75 $ in cases 2, 3 and 4, respectively. Table II depicts the cost of scheduled and deployed reserves of MG in different cases. Through incorporating DR activities, the scheduled reserve capacity can be provided by DG units (including up-, down- and non-spinning reserve) as well as responsive loads (including up- and down-spinning reserve). As mentioned, the MG reserves are managed by MGCC in a way to minimize the operational cost of MG while satisfying the system constraints. In other word, MGCC would be responsible to determine the contribution of reserve capacity provided by DG units and DR resources, economically to assure power balance under any working condition. Without applying DR program, the costs of scheduled and deployed reserves are 174.75 $ and -102.68 $, respectively. But, as it can be observed from Table II, by increasing DR activities, the cost of scheduled reserve is decreased in all cases as provision of reserve service is partially done by responsive loads at lower prices. Also, with increasing DR participation, cost of deployed reserves by DG units in real-time to accommodate the uncertainties is decreased. It should be noted that, the minus sign of the deployed reserves cost is interpreted as the expected profit of the MG operator. The simulation results show that with applying proposed approach the system frequency is regulated well enough around the nominal value (i.e. 60 Hz) through optimal coordination of DERs and DR actions based on a meaningful trade-off between technical and economical issues. In order to provide more elaboration about the system frequency security, it is analyzed in two worst case scenarios in this section. The highest frequency drop is related to scenario 21 where demand level and RESs generation have their maximum and minimum values, respectively. The other extreme case happens in scenario 5 where the load consumption and RESs generation have their minimum and maximum levels, respectively and the system frequency jumps to the highest value. The frequency profiles regarding the scenario 5 at 10% and 40% DR participants for all cases during 24 hours of the scheduling time horizon are depicted in Fig. 4. As shown in Fig. 4-(a), in case 1, the frequency excursion is at the maximum allowable value (i.e. 60.36 Hz). But with 10% DR participants, due to the reduction of customers' consumption, especially during peak hours, the frequency excursion reduces and remains within a secure range. Because, with consideration of DR influence on frequency regulation, the difference between DGs generation level and their power set-points is lower than that of in case 1, so, the frequency deviations are relatively higher in the cases with DR. As it can be observed from Fig. 4-(b), with increasing DR participants, due to the higher contribution of responsive loads in frequency regulation, its standard deviation in this condition is relatively. In case 4, both sheddable and shiftable loads participate in DR and as the result, system frequency security has better conditions in comparison with other cases.

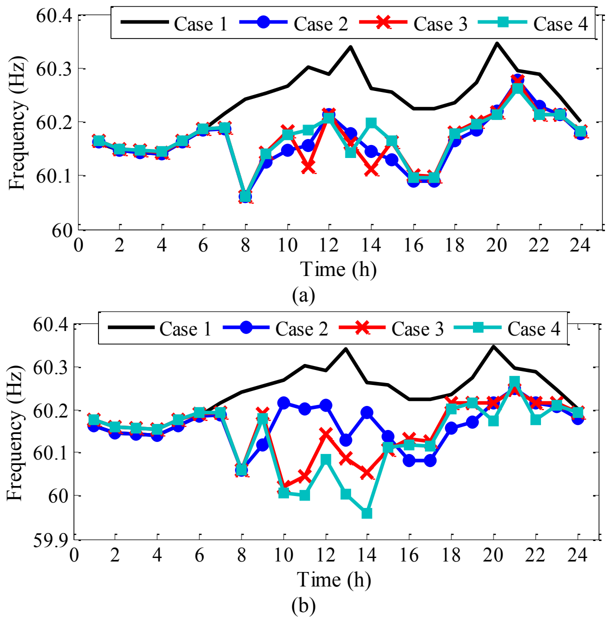

Fig. 4. Hourly frequency profiles of different cases in scenario 5, (a) 10% DR participants, and (b) 40% DR participants.

The frequency profiles in scenario 21 are shown in Fig. 5. As observed, in this scenario the frequency drops severely because of the demand load has its highest value. As depicted in Fig. 5, the frequency security is improved relatively better in case 2 than the other cases due to the fact that some of the loads are curtailed and as the result, low inertia units are not committed. In addition, it can be also observed that with active participation of end-users in DR programs, especially during peak hours, the system frequency goes under less variation as more reserve is allocated by responsive loads. It should be noted that, in this study in order to evaluate the frequency security, the worst scenarios (i.e., scenarios 5 and 21) are analyzed. These scenarios represent the frequency deviation in worst case scenarios with a probability of occurrence which is very low (i.e., 0.0041). The results show that the frequency deviations in other scenarios are lower than the mentioned scenarios.

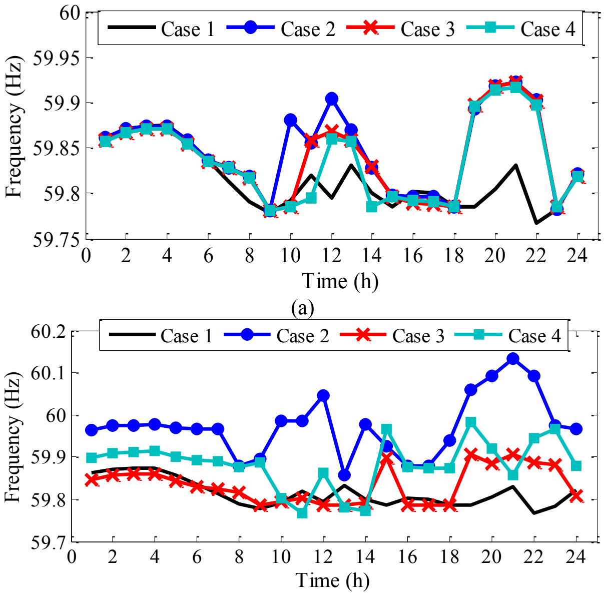

(b)

Fig. 5. Hourly frequency profiles of different cases in scenario 21, (a) 10% DR participants, and (b) 40% DR participants.

V. Conclusions

This paper presented a stochastic model for frequency security-constrained unit commitment associated with DR actions. In the proposed model the MG frequency security was managed by MGCC in order to maximize the expected profit of MGO. The MGCC also adjusted the power set-points of DR and DG resources such that not only the steady-state frequency was assured but also the customers' payment was minimized. To study the uncertainties of load consumption and RESs productions, a scenario-based stochastic programming method was also employed. Moreover, an AC-optimal power flow (AC-OPF) approach was applied to model the actual operating conditions and to determine the effect of DR programs on frequency security in steady state. The numerical results revealed that customers' participation in energy and reserve scheduling, have a great impact on the MG frequency security provision. It was also demonstrated that with the application of DR programs, the frequency deviation could be reduced significantly and the DG capacities could be managed with higher degrees of freedom.

References

[1] R. Sharifi, A. Anvari-Moghaddam, S. H. Fathi, J.M. Guerrero, V. Vahidinasab, "An Economic Demand Response Model in Liberalized Electricity Markets with Respect to Flexibility of Consumers", IET Gener. Trans. Dist., 2017, DOI: 10.1049/iet-gtd.2017.0412.

[2] A. Anvari-Moghaddam, J.C. Vasquez, J.M. Guerrero, "Load Shifting Control and Management of Domestic Microgeneration Systems for Improved Energy Efficiency and Comfort", 41st Annual Conference of the IEEE Industrial Electronics Society (IECON'15), November 9-12, Yokohama, Japan, 2015, pp. 96-101.

[3] M.Vahedipour-Dahraie, H. R.Najafi, A. Anvari-Moghaddam, and J. M. Guerrero, "Study of the Effect of Time-Based Rate Demand Response Programs on Stochastic Day-Ahead Energy and Reserve Scheduling in Islanded Residential Microgrids," Appl. Sci., vol. 7, no. 4, pp. 1-19, 2017.

[4] M. Vahedipour-Dahraie, A. Anvari-Moghaddam, J.M. Guerrero, "Evaluation of Reliability in Risk-Constrained Scheduling of Autonomous Microgrids with Demand Response and Renewable Resources", IET Renew. Power Gener., 2018. DOI: 10.1049/iet-rpg.2017.0720.

[5] R. Sharifi, A. Anvari-Moghaddam, S. H. Fathi, J.M. Guerrero, V. Vahidinasab, "Dynamic Pricing: An Efficient Solution for True Demand Response Enabling", J. Renew. Sustain. Energy, vol. 9, no. 6, pp.1-14, 2017.

[6] A. Anvari-Moghaddam, H. Monsef, and A. Rahimi-Kian, "Cost-Effective and Comfort-Aware Residential Energy Management under Different Pricing Schemes and Weather Conditions," Energy and Buildings, vol. 86, pp. 782-793, 2015.

[7] A. Gholami, T. Shekari, F. Aminifar, and M. Shahidehpour, "Microgrid Scheduling with Uncertainty: The Quest for Resilience," IEEE Trans smart grid, vol. 30, no. 3, pp. 1337-1350, 2016.

[8] A. Moshari, A. Ebrahimi, and M. Fotuhi-Firuzabad, "Short-Term Impacts of DR Programs on Reliability of Wind Integrated Power Systems Considering Demand-Side Uncertainties," IEEE Trans on Power Syst. Vol. 31, no. 3, pp. 2481-2490, 2016.

[9] M. M. A., Abdolaziz, and E. F. El-Saadany, "Maximum loadability consideration in droop controlled islanded microgrids optimal power flow," Electric Power Syst. Res., vol. 106, pp.168-179, 2014.

[10] E. Rodriguez-Diaz, E.J. Palacios-Garcia, A. Anvari-moghaddam, J.C. Vasquez, J.M. Guerrero, "Optimal Management of a hybrid AC/DC Residential Microgrid", 2nd IEEE International Conference On DC Microgrids (ICDCM 2017), June 27-29, Nürnberg, Germany, 2017.

[11] H. Han, S. Gao, Q. Shi, H. Cui and F. Li, "Security-Based Active Demand Response Strategy Considering Uncertainties in Power Systems," in IEEE Access, vol. 5, pp. 16953-16962, 2017.

[12] J. Aghaei, A. Ahmadi, A. Rabiee, V.G. Agelidis, K.M. Muttaqi, and H. Shayanfar, "Uncertainty management in multiobjective hydro-thermal self-scheduling under emission considerations," Appl. Soft Comput. Vol. 37, pp. 737-750, 2015.

[13] G. Carpinelli, R. Rizzo, P. Caramia, and P. Varilone, "Taguchi's method for probabilistic three-phase power flow of unbalanced distribution systems with correlated Wind and Photovoltaic Generation Systems", Renewable Energy, vol. 117, pp. 227-241, 2018.

[14] M. Zachar and P. Daoutidis, "Microgrid/Macrogrid Energy Exchange: A Novel Market Structure and Stochastic Scheduling," IEEE Trans. on Smart Grid, vol. 8, no. 1, pp. 178-189, 2017.

[15] N. Rezaei, and M. Kalantar, "Smart microgrid hierarchical frequency control ancillary service provision based on virtual inertia concept: An integrated demand response and droop controlled distributed generation framework," Energy Conversion and Management, vol. 92, pp. 287-301, 2015.

[16] H.T. Haider, O.H. See, and W. Elmenreich, "A review of residential demand response of smart grid," Renew. Sustain. Energy Rev.vol. 59, pp. 166-178, 2016.

[17] A. Anvari-Moghaddam, H. Monsef, A. Rahimi-Kian, and H. Nance, "Feasibility Study of a Novel Methodology for Solar Radiation Prediction on an Hourly Time Scale: A Case Study in Plymouth," UK. J Renew & Sustain Energy, vol. 6, pp. 331-337, 2014.

[18] I.G. Damousis, A.G. Bakirtzis, and P.S. Dokopolous, "A solution to the unit-commitment problem using integer coded genetic algorithm," IEEE Trans. Power Syst., vol. 19, no. 2, pp. 1165-1172, 2004.

[19] D. Arthur, and S. Vassilvitskii, "K-means++: The advantages of careful seeding," in Proc. 18th Annu. ACM-SIAM Symp Discrete Algorithms (SODA '07) ', New Orleans, LA, USA, 2007, pp. 1027-1035

[20] M. Vahedipour-Dahraie, H. Rashidizaheh-Kermani, H.R.. Najafi, A. Anvari-Moghaddam, and J. M. Guerrero, "Stochastic Security and Risk-Constrained Scheduling for an Autonomous Microgrid with Demand Response and Renewable Energy Resources," IET Renewable Power Generation, vol. 11, npo. 14, pp. 1812-1821, 2017.